Hierarchical Control of Parallel AC-DC Converter Interfaces for Hybrid Microgrids

Lu, Xiaonan; Guerrero, Josep M.; Sun, Kai; Vasquez, Juan Carlos; Teodorescu, Remus; Huang, Lipei

Published in:
I E E E Transactions on Smart Grid

DOI (link to publication from Publisher):
10.1109/TSG.2013.2272327

Publication date:
2014

Document Version
Early version, also known as pre-print

Hierarchical Control of Parallel AC-DC Converter Interfaces for Hybrid Microgrids

Xiaonan Lu, *Student Member, IEEE*, Josep M. Guerrero, *Senior Member, IEEE*, Kai Sun, *Member, IEEE*, Juan C. Vasquez, *Member, IEEE*, Remus Teodorescu, *Fellow, IEEE*, Lipei Huang

***Abstract*-- In this paper, a hierarchical control system for parallel power electronics interfaces between ac bus and dc bus in a hybrid microgrid is presented. Both standalone and grid-connected operation modes in the dc side of the microgrid are analyzed. Concretely, a three-level hierarchical control system is implemented. In the primary control level, the decentralized control is realized by using the droop method. Local ac current proportional-resonant controller and dc voltage proportional-integral controller are employed. When the local load is connected to the dc bus, dc droop control is applied to obtain equal or proportional dc load current sharing. The common secondary control level is designed to eliminate the dc bus voltage deviation produced by the droop control, with dc bus voltage in the hybrid microgrid boosted to an acceptable range. After guaranteeing the performance of the dc side standalone operation by means of the primary and secondary control levels, the tertiary control level is thereafter employed to perform the connection to an external dc system. Meanwhile, the impact of the bandwidth of the secondary and tertiary control levels is discussed. The closed-loop model including all the three control levels is developed in order to adjust the main control parameters and study the system stability. Experimental results of a 2×2.2 kW parallel ac-dc converter system have shown satisfactory realization of the designed system.**

***Index Terms* - Hierarchical control, hybrid microgrid, parallel power electronics converter interface**

I. Introduction

Nowadays renewable energy generation is expected to be highly penetrated into modern electric grids [1-2]. In order to integrate different kinds of renewable energy sources, the concept of microgrid was proposed several years ago [3]. Meanwhile, power electronics converters are usually used as the interfaces to connect each source to the common bus in a microgrid [4-6]. At the same time, ac and dc sources sometimes coexist in a practical microgrid. In order to deal with that, ac-dc hybrid microgrids have been studied in the literature [7-8]. It is necessary to find effective control systems to facilitate the proper interaction between ac and dc buses in hybrid microgrids.

Since the distributed renewable energy sources can be connected into a microgrid separately, the interfacing converters are usually connected in parallel. With the parallel configuration, the load power sharing among the converters has been a key research topic [9-13]. The output power should be appropriately shared based on the power ratings of each converter. Various power sharing methods have been proposed and analyzed. Centralized control method is proposed in [14], where a central controller is adopted to give the current reference to each converter. Master-slave control in [15] performs a combination of one voltage-controlled converter and several current-controlled converters. The voltage-controlled converter generates the current reference for the other current-controlled converters. In [16], a method named circular-chain-control (3C) is proposed, where the converters are cascade connected and each converter generates the current reference for the adjacent one. Average current control method is shown in [17]. With the method, the current references are generated and transferred to each converter through a communication line. By using the above methods, although the steady and dynamic performance of current sharing can be guaranteed, the stability of the control system highly depends on high speed communications. The system redundancy is lowered down and the maintenance cost is higher. Meanwhile, considering the distributed configuration of a microgrid, the decentralized control method or the control method based on low bandwidth communication (LBC) is more suitable for microgrid applications. Therefore, the droop control method has been commonly employed to perform proper current sharing in a microgrid [10-13]. With droop control, decentralized control for each interfacing converter is achieved. At the same time, no communication or only LBC is needed.

Among different communication methods, the local area network (LAN)/Ethernet and the optical fiber transmission can be used for the implementation of high bandwidth communication (HBC). However, additional cost is needed to achieve the infrastructure for this communication method [18-19]. Controller area network (CAN) can be used as the LBC method [20]. Particularly, when the transmission distance becomes longer, the communication speed of CAN becomes lower. Meanwhile, for LBC method, in ac systems, power line communication (PLC) can be used [21], and PLC in dc

This work was supported by the National Natural Science Foundation of China (51177083) and China Scholarship Council.

X. Lu, K. Sun and L. Huang are with the State Key Lab of Power Systems, Department of Electrical Engineering, Tsinghua University, Beijing, 100084, China.

J. M. Guerrero, J. C. Vasquez and R. Teodorescu are with the Institute of Energy Technology, Aalborg University, 9220, Denmark.

K. Sun is the corresponding author. Postal address: 3-310, West Main Building, Tsinghua University, Beijing, China. Telephone number: 86-10-62796934. Email: sun-kai@mail.tsinghua.edu.cn.

systems has been also developed [22].

As ac power system is mainly utilized nowadays, more attention is on ac microgrid [23-24]. However, many kinds of renewable energy sources have dc output, such as photovoltaic (PV) modules and batteries. As aforementioned, both dc and ac components usually coexist in one system. Therefore, they can form a hybrid microgrid. Different control methods of hybrid microgrids have been proposed in the literature. Droop control is employed in [7] and the controllable loads with different capacities are taken into account. A coordinate control method for a hybrid microgrid composed of various kinds of renewable energy sources is proposed in [8], where detailed models of PV modules, batteries and wind turbines are derived and the energy management strategy for the whole system is developed. A configuration with both dc and ac links and the corresponding control method are presented in [25], where the dc-link is employed to integrate the local converters with dc couplings and it is connected to the common ac-link through dc-ac interfacing converters. A power quality enhancement method is proposed in [26], where the unbalanced and nonlinear loads are taken into account and the control strategy is developed in a multi-bus microgrid. The above methods are useful to enhance the performance of a hybrid microgrid. However, they mainly focus on the ac side of the system. A typical ac-dc hybrid microgrid consists of three main parts: (I) ac microgrid, (II) dc microgrid and (III) power electronics interfaces between ac and dc buses. In [27], a generalized droop control method is proposed to achieve the proper power sharing in different parts of a hybrid microgrid, while the deviation produced by droop control should be further eliminated and the control of the power exchange between the local and external grids should be discussed. In [28], the control systems of ac microgrids and dc microgrids are analyzed and a hierarchical control system is developed. However, in the work related to the dc microgrids, only the basic simulation results based on parallel buck converters are shown. Meanwhile, the operation of the interfacing converters between ac and dc buses is not included.

This paper accomplishes an extension of the hierarchical control system with the discussion of different operation modes, especially for the interfacing converters between ac and dc buses in a hybrid microgrid. Meanwhile, the impact of the LBC on the system stability is studied in detail. Concretely, the hierarchical control system for the interfacing power electronics converters consists of three levels. In the primary level, distributed control is realized. Current proportional-resonant (PR) controller and voltage proportional-integral (PI) controller are achieved individually in each of the converters. Droop controller for dc current sharing is also employed. In the secondary control level, the dc voltage deviation produced by droop control is eliminated. In order to realize current sharing between parallel droop-controlled converters, there is a tradeoff between current sharing accuracy and dc voltage deviation [29]. The target of the secondary PI controller is to restore the voltage deviation and maintain the current sharing accuracy. Both the primary and secondary levels of the hierarchical control system are employed in the dc-side standalone operation mode. In order to control the power exchange between local dc bus and other external dc grids, the PI controller in the tertiary control level is used. It should be noticed that both secondary and tertiary control levels have remarkable low bandwidth characteristics, which guarantee that the bandwidth will not interfere with the decentralized controllers in the primary control level for each converter. The performance of the control system with different communication bandwidth is validated by experiment in detail in this paper.

II. Classification of Different Operation Modes in a Hybrid AC-DC Microgrid

As aforementioned, an ac-dc hybrid microgrid consists of three parts: ac microgrid, dc microgrid and multiple parallel interfaces between ac and dc buses. Considering the configuration of the ac-dc hybrid system, different operation modes and their power flow patterns are shown in Fig. 1.

Mode (a) and (b) are the operation modes of pure ac microgrid and dc microgrid, respectively. Mode (c) and (d) are the operation modes considering the interfacing converters between ac and dc buses. In Mode (a), the ac loads are supplied by the sources in the ac side. Meanwhile, when the ac grid-connected static switch turns on, the power in the local microgrid exchanges with the external ac grid. In Mode (b), the local dc loads are supplied by the sources in the dc side. When the dc grid-connected static switch turns on, the power in the local microgrid exchanges with the external dc grid. In Mode (c), the ac loads are supplied by the sources in the dc side. When the system turns to grid-connected mode, the power exchanges between the dc-side sources and external ac grid. In Mode (d), the dc loads are supplied by the sources in the ac side. When turning into grid-connected mode, the power exchanges between the ac-side sources and external dc grid. Notice that the practical operation modes can be regarded as the composition of the above four basic operation modes.

Hierarchical control systems of Mode (a) and (b) have already been discussed in [28]. In Mode (c), the dc bus voltage is kept stable by controlling the converters in the dc microgrid. This is out of scope of this paper since it is essentially from dc to ac and the control system is equivalent to Mode (a). The different operation modes and the usage of the hierarchical control system in a hybrid microgrid are summarized in Table I.

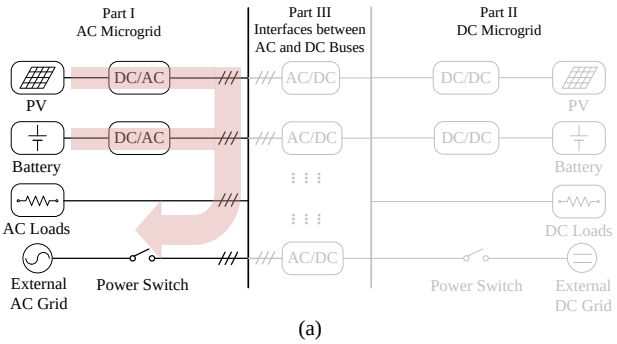

(a)

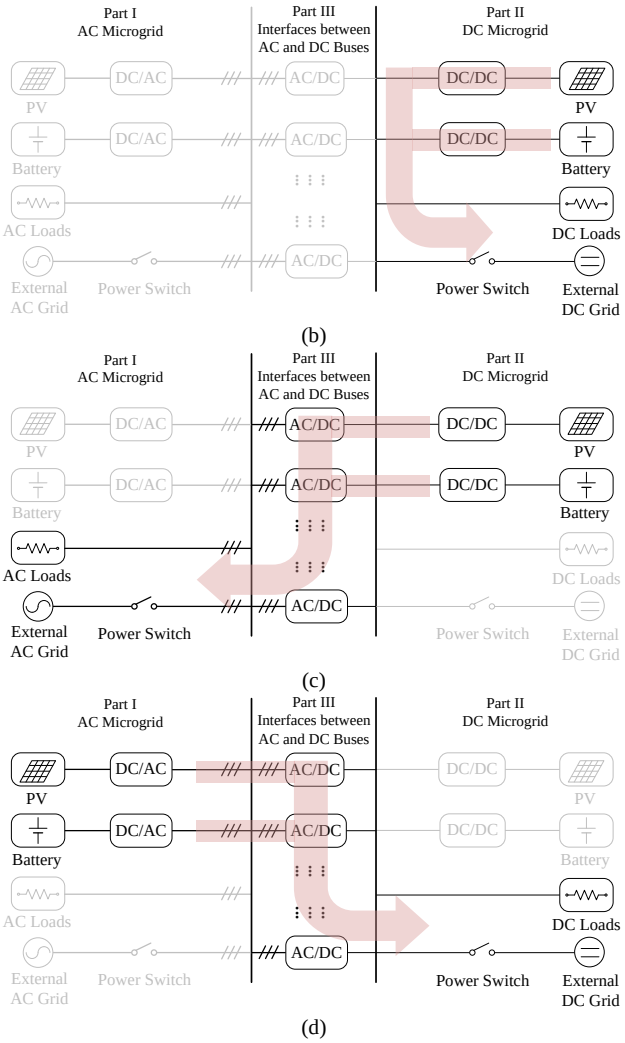

Fig. 1. Different operation modes and the corresponding power flow in an ac-dc hybrid microgrid.
(a) AC microgrid operation. (b) DC microgrid operation. (c) Hybrid microgrid operation with dc to ac power flow. (d) Hybrid microgrid operation with ac to dc power flow.

This paper focuses on Mode (d). In Mode (d), if considering the operation of dc/dc converters in the dc microgrid part, since the dc bus voltage is formed by controlling the parallel interfacing converters between ac and dc buses, the renewable energy sources in the dc microgrid, e.g. PVs, which commonly run in MPPT mode, operate in current-controlled mode to behave as grid-connected modules and inject its maximum output power into the dc bus. Meanwhile, the energy storage units in the dc microgrid operate in voltage-controlled mode and *I-V* droop control method is also employed in their control systems. In Mode (d), the power flows from the ac side to the dc side. Since the power generation in the ac microgrid is more sufficient than that in the dc microgrid, the interfacing converters between ac and dc buses are selected to form the dc bus voltage.

If considering the operation of dc/ac converters in the ac microgrid part, similar to the converter control in the dc microgrid part, the renewable energy sources, such as PVs, also operate in current-controlled mode to behave as grid-connected modules and inject its maximum power into the ac bus. Meanwhile, the energy storage units operate in voltage-controlled mode and *P-f* / *Q-V* droop control method is used for them [11]. Since in Mode (d), sufficient power is generated in the ac microgrid part, the ac bus voltage is formed by the energy storage units in the ac side. The deviation produced by droop control is eliminated by employing secondary control in the control system for the energy storage units in the ac microgrid part. In this way, the ac bus voltage can be formed to stabilize the input of the interfacing converters between ac and dc buses.

It should be noted that since the research subject is focused on the interfacing converters between ac and dc buses in this paper, only the analysis of the hierarchical control system for this part is performed in detail.

III. Design and Evaluation of the DC-Side Hierarchical Control System for the Interfacing Converters between AC and DC Buses

In order to enhance the performance of the parallel power electronics interfaces for Mode (d) in Fig. 1, a dc-side hierarchical control system is implemented, as shown in Fig. 2, and the function and characteristic of each control level is shown in Table II. Concretely, local dc voltage and ac current controller is included in the primary level. Also in the distributed primary control level, dc output current sharing is achieved by using droop controller. In the secondary control level, the deviation caused by the droop control is eliminated. The dc bus voltage is boosted to the acceptable range. DC grid-connected current is controlled in the tertiary control level. The detailed design and evaluation of the whole dc-side hierarchical control system is shown below.

A. Primary control level

In the primary control level, the conventional double loop control diagram is employed first, including the inner ac current loop and outer dc voltage loop. PR controller is used for ac current control, and PI controller is used for dc voltage control. The above controllers are shown as

$$G_{\mathrm{pr\_p}} = K_{\mathrm{pc\_p}} + \frac{K_{\mathrm{rc\_p}}}{s} \tag{1}$$

where $G_{\mathrm{pr\_p}}$ is the transfer function of the PR controller for ac current in the primary control level, $K_{\mathrm{pc\_p}}$ and $K_{\mathrm{rc\_p}}$ are the parameters of the proportional and resonant terms respectively.

$$G_{\mathrm{pi\_p}} = K_{\mathrm{pv\_p}} + \frac{K_{\mathrm{iv\_p}}}{s} \tag{2}$$

where $G_{\mathrm{pi\_p}}$ is the transfer function of the PI controller for dc voltage in the primary control level, $K_{\mathrm{pv\_p}}$ and $K_{\mathrm{iv\_p}}$ are the parameters of the proportional and integral terms respectively.

Since the above PR and PI controllers have the common form, no more descriptions are shown here for brevity.

In order to reach proper load power sharing in the dc side, droop control is employed. The reference value of the dc output voltage is obtained by using *I-V* droop curve, as shown in Fig. 3, where v_{dcmax} and v_{dcmin} are the upper and lower boundaries of local dc voltage, $v_{\mathrm{dc(margin)}}$ is the design margin, and R_{d} is the virtual resistance.

TABLE I
Summary of Different Operation Modes

	AC - Side Sources	DC - Side Sources	Power Flow	Control System		
				Primary Level	Secondary Level	Tertiary Level
Mode (a)	√	×	DC sources → AC loads and grid	Control of ac voltage/ac current AC load sharing	AC voltage restoration	Connection to external ac grid
Mode (b)	×	√	DC sources → DC loads and grid	Control of dc voltage/dc current DC load sharing	DC voltage restoration	Connection to external dc grid
Mode (c)	×	√	DC sources → AC loads and grid	Control of ac voltage/ac current AC load sharing	AC voltage restoration	Connection to external ac grid
Mode (d)	√	×	**AC sources → DC loads and grid**	**Control of ac current/dc voltage DC load sharing**	**DC voltage restoration**	**Connection to external dc grid**

√: sources available ×: sources not available

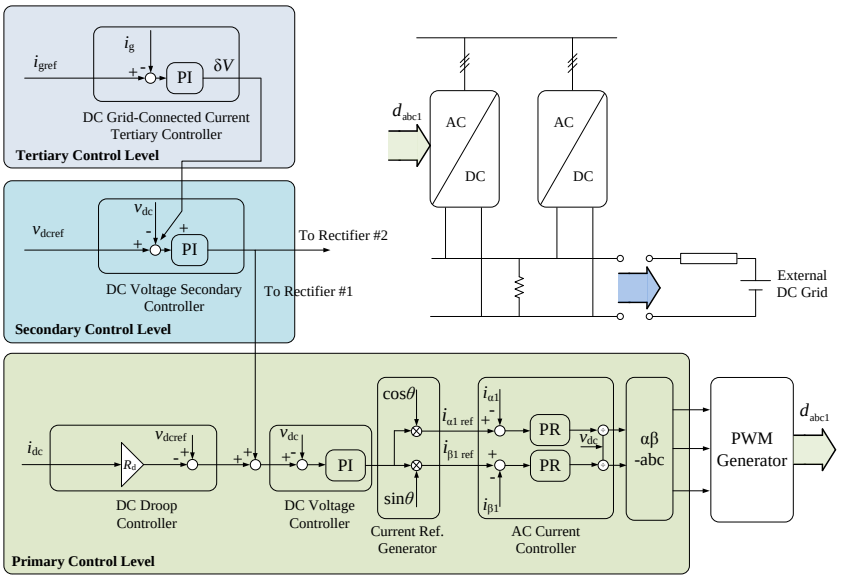

Fig. 2. DC-side hierarchical control diagram.

The dc side droop control method can be expressed as

$$v_{dc} = v_{dcref} - i_{dc}R_d \tag{3}$$

As mentioned above, by using droop control, the dc voltage deviation is involved, which makes the dc voltage quality lowered down. Hence, the value of the virtual resistance R_d should not be so large that v_{dc} can be kept within the acceptable range, as shown as

$$R_d \le [(v_{dcmax} - v_{dc(margin)}) - (v_{dcmin} + v_{dc(margin)})] / I_{dc(FL)} \tag{4}$$

where $I_{dc(FL)}$ is the full load current in the dc side.

TABLE II
Function and Characteristic of Each Control Level

	Function	Characteristic
Primary Level	Local ac current and dc voltage control, droop control	Decentralized
Secondary Level	Common dc-bus voltage control	LBC
Tertiary Level	Common dc-side grid-connected current control	LBC

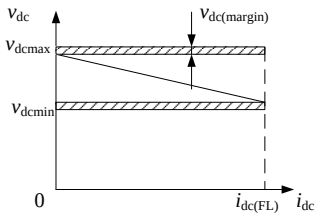

Fig. 3. DC voltage deviation caused by droop control.

In order to realize both equal and proportional current sharing, the corresponding droop control relationship can be realized as

$$\begin{cases} v_{dc1} = v_{dcref} - i_{dc1}R_{d1} \\ v_{dc2} = v_{dcref} - i_{dc2}R_{d2} \end{cases} \tag{5}$$

If neglecting the line resistances,

$$v_{dc1} = v_{dc2} \tag{6}$$

Hence, it can be derived that

$$i_{dc1} / i_{dc2} = R_{d2} / R_{d1} \tag{7}$$

It means that equal or proportional dc load current sharing can be achieved by using equal or proportional virtual resistance respectively.

B. Secondary control level

The secondary control level consists of a common dc voltage PI controller. This control loop has remarkable low bandwidth characteristic. With the secondary controller, the dc voltage deviation produced by droop control in the primary control level can be restored, as shown in Fig. 4.

The secondary control features are analyzed in this subsection. The control diagram, including primary control,

secondary control and a delay block are shown in Fig. 5. Here, the transfer function of the PI controller in the primary control level is shown in (2). Meanwhile, the PI controller in the secondary control level is shown as:

$$G_{\text{pi\_s}} = K_{\text{pv\_s}} + \frac{K_{\text{iv\_s}}}{s} \tag{8}$$

where $G_{\text{pi\_s}}$ is the transfer function of the PI controller for common dc bus voltage in the secondary control level, $K_{\text{pv\_s}}$ and $K_{\text{iv\_s}}$ are the parameters of the proportional and integral terms respectively.

G_{delay}, G_{current} and G_{plant} represent the transfer functions of the communication delay, the current loop in the primary control level and the power plant, respectively. Among them, G_{delay} is expressed as

$$G_{\text{delay}} = \frac{1}{1+\tau \cdot s} \tag{9}$$

where the parameter τ represents the time delay in this control level, which is used to simulate different communication bandwidth.

Since the current loop is the inner control loop of the primary control level and the bandwidth of the inner loop is much higher than the outer loop, G_{current} is simplified as a delay unit for one control period, as shown below in (10).

$$G_{\text{current}} = \frac{1}{1+T_{\text{d}} \cdot s} \tag{10}$$

where T_{d} is the control period.

In order to form the feedback channel in the secondary dc voltage loop, G_{plant} is employed to show the relationship from the inner loop current to the dc voltage. It can be achieved by using the small signal analysis, as shown in [30]. Neglecting the losses in the converter, the active power in the ac side can be considered to be the same as that in the dc side. By analyzing the circuit in Fig. 6, the following relationship can be reached.

$$e_{\text{d}} i_{\text{d}} + e_{\text{q}} i_{\text{q}} = v_{\text{dc}} \cdot C_{\text{dc}} \frac{\text{d}v_{\text{dc}}}{\text{d}t} + v_{\text{dc}} i_{\text{L}} \tag{11}$$

where e_{d} and e_{q} are the ac voltage, i_{d} and i_{q} are the ac current, v_{dc} is the dc voltage, C_{dc} is the dc capacitor, and i_{L} is the dc load current.

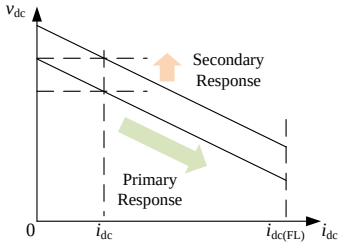

Fig. 4. Effect of secondary control on dc voltage restoration.

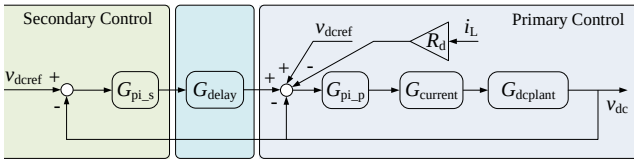

Fig. 5. Control diagram of the secondary control level.

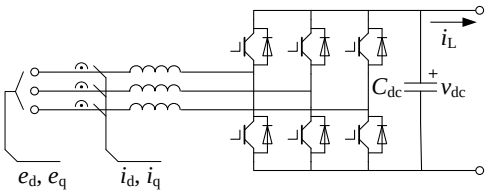

Fig. 6. Detailed structure of the AC-DC power interface.

The small signal expression of (11) can be derived as

$$\begin{aligned}&(E_{\text{d}}+\hat{e}_{\text{d}})(I_{\text{d}}+\hat{i}_{\text{d}})+(E_{\text{q}}+\hat{e}_{\text{q}})(I_{\text{q}}+\hat{i}_{\text{q}})\\&=(V_{\text{dc}}+\hat{v}_{\text{dc}})\cdot C_{\text{dc}}\frac{\text{d}(V_{\text{dc}}+\hat{v}_{\text{dc}})}{\text{d}t}+(V_{\text{dc}}+\hat{v}_{\text{dc}})(I_{\text{L}}+\hat{i}_{\text{L}})\end{aligned} \tag{12}$$

Since v_{dc} is controlled by the current component i_{d}, the other perturbations can be neglected and the transfer function from i_{d} to v_{dc} is obtained:

$$G_{\text{dcplant}} = \frac{\hat{v}_{\text{dc}}}{\hat{i}_{\text{d}}} = \frac{E_{\text{d}}}{sC_{\text{dc}}V_{\text{dc}} + I_{\text{L}}} \tag{13}$$

It should be noted that the analysis in the rotating frame with the variables in the d and q axis is employed only to derive the transfer function of G_{dcplant} in (13). The ac current controllers adopted in the primary control level of the hierarchical control system are realized in the stationary frame, with the variables in the α and β axis.

By using the system parameters in Table III, the closed-loop poles of the whole system with increasing time delay are reached in Fig. 7, where only dominant poles are shown. The location of different closed-loop poles is determined by changing the value of the communication delay.

The trajectory of the dominant poles with different time delay is divided into three parts. When the time delay becomes larger, the dominant pole λ_1 is moving towards its final point P_{I}. It can be seen that the whole trajectory of λ_1 is located on the left half plane. At the same time, when the time delay turns larger, λ_2 and λ_3 are moving gradually towards imaginary axis. It should be pointed out that even the delay is as large as 0.2 s, λ_2 and λ_3 are -1.6 ± j7.6. Therefore, the system has enough stability margins and the low bandwidth characteristic of the secondary control level is verified. Notice that the root λ_1, which moves faster towards the imaginary axis than λ_2 and λ_3, ends at the point P_{I}. For some communication delays, only λ_2 and λ_3 are dominants and the effect of λ_1 can be neglected.

C. Tertiary control level

The above primary and secondary control levels are employed in the dc-side standalone operation mode. With the progress of distributed generation, areas with multiple microgrid clusters can be found. In this situation, similar to that in an ac microgrid, it is useful to pay attention to the interaction in the dc side between the local microgrid and external dc grid. The seamless transfer between dc standalone and grid-connected operation modes should be guaranteed. In order to meet this requirement, a tertiary control level in the dc-side hierarchical control system is employed. In this control level, as same as that in the secondary control level, a common dc grid current PI controller is used. This control level also has remarkable low bandwidth characteristic. The target of tertiary

control is to realize dc grid-connected current control. Concretely, dc load sharing is firstly achieved by the droop controller in the decentralized primary control level. And then, secondary control is employed to restore the deviation produced by droop control. When the difference between dc output voltage and dc grid voltage are within the acceptable range, the static switch for grid-connected operation is turned on. At the same time, the tertiary control level is activated to control the dc grid-connected current.

The features of tertiary control level are analyzed in this subsection. The control configuration of this control level is shown in Fig. 8, where both the primary and secondary control levels are included. A delay block is also cascade connected with the tertiary PI controller to model the LBC. Here, by using the system parameters in Table III, the dominant poles with increasing time delay are shown in Fig. 9. It is seen that the trajectory of the dominant poles can be divided into four parts. When the time delay increases, the dominant poles λ_1 and λ_2 move gradually away from the imaginary axis. Meanwhile, the dominant poles λ_3 and λ_4 move towards the imaginary axis, while even the time delay is as large as 1 s, λ_3 and λ_4 are -0.1 ± j0.5, respectively. Therefore, the system has acceptable stability margins and the low bandwidth characteristic of the tertiary control level is demonstrated.

TABLE III
System Parameters

Item	Value	Unit
AC Voltage (rms)	230	V
AC Frequency	50	Hz
DC Ref. Grid-Connected Current (In Tertiary Level)	1	A
DC Load	400	Ω
DC Line Inductance	1.8	mH
DC Line Resistance	2	Ω
AC Filter Inductance	1.8	mH
AC Filter Capacitor	4.7	μF
DC Bus Capacitor	600	μF

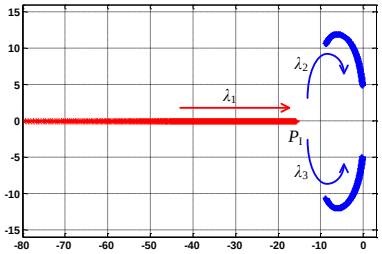

Fig. 7. Family of the closed-loop poles of the secondary control level when increasing the time delay.

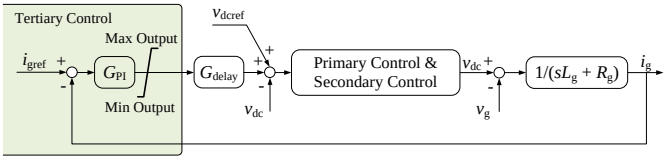

Fig. 8. Control diagram of the tertiary control level.

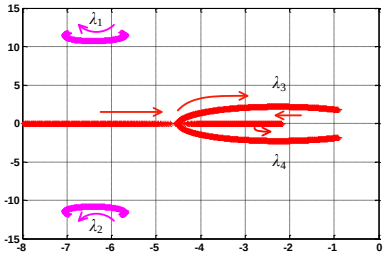

Fig. 9. Family of the closed-loop poles of the tertiary control level when increasing the time delay.

Notice that when the communication delay increases, λ_1 and λ_2 move away from the imaginary axis, while λ_3 and λ_4 move towards the imaginary axis. For some communication delays, λ_3 and λ_4 are dominants, and the effect of λ_1 and λ_2 can be neglected.

It should be guaranteed that the local dc voltage is maintained in the acceptable range, not only in the standalone mode but also in the grid-connected mode. Since the output of the tertiary controller is added into the dc voltage reference value and PI controller is employed in the secondary control level, it is reached in the steady state that

$$v_{\mathrm{dcref}} + \delta v = v_{\mathrm{dc}} \tag{14}$$

where v_{dcref} is the reference value of dc bus voltage, δv is the output value of tertiary PI controller.

Therefore, the local dc voltage will be shifted by δv when the system is operated in the grid-connected mode. As a result, δv should be limited within the acceptable range. Assuming that the dc reference voltage is 600V and the maximum dc voltage error is 5%, the maximum and minimum δv are thereby confirmed as ±30V, which are the PI output upper and lower limits of the tertiary control (see Fig. 8).

As a summary of the design for the dc-side hierarchical control system, all parameters of the controllers are listed in Table IV.

D. Interaction between different control levels

In the above design procedure of the hierarchical control system, the inner control level has been taken into account when designing the outer control level. At the same time, the influence of the inner control level has been considered when adjusting the controller parameters in the outer levels.

In order to study the interaction between different control levels, the dominant poles of the whole control system are shown in Fig. 10. It can be seen that when going from lower to upper levels, the system dynamics become slower. Furthermore, the natural frequencies of the dominant poles of each control level are separated between each other by about one decade (primary: -15, secondary: -1.6 ± j7.6 and tertiary: –0.1 ± j0.5). Consequently, it can be concluded that each control level do not affects the dynamics of the others.

IV. Experimental Validation

A 2×2.2 kW prototype of parallel converter interface for experimental validation was implemented. The detailed configuration of the experimental setup is shown in Fig. 11.

The parameters of the system are the same as those chosen in the theoretical analysis, as listed in Table III.

TABLE IV
Controller Parameters of the DC-side Hierarchical Control System

Item		Value	Unit
Primary Control Level			
AC Current Controller	Proportional Term	16	-
	Resonant Term	2000	-
DC Voltage Controller	Proportional Term	1.3	-
	Integral Term	6	-
Droop Controller		6	Ω
Communication Bandwidth		Decentralized	
Secondary Control Level			
DC-Bus Voltage Controller	Proportional Term	0.003	-
	Integral Term	13	-
Communication Bandwidth		500	Hz
Tertiary Control Level			
DC Current Controller	Proportional Term	0.6	-
	Integral Term	20	-
Communication Bandwidth		250	Hz

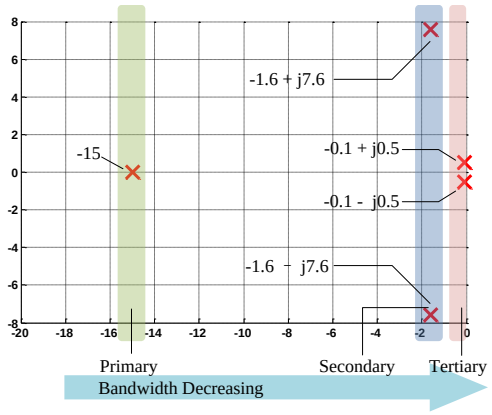

Fig. 10. Dominant poles of different control levels.

In the primary control level, voltage and current controllers are tested first without droop control. The local dc voltage waveform is shown in Fig. 12 and the corresponding local ac current response is shown in Fig. 13. Then, droop control is verified. When droop controller is activated, the dc current is equally shared, while the deviation in the dc voltage appears, as shown in Fig. 14 and 15. After testing equal dc sharing, proportional dc current sharing is performed. When R_{d1}=6Ω and R_{d2}=12Ω, *I-V* curve for proportional current sharing is drawn in Fig. 16. For a certain value of dc voltage, the corresponding current values of Converter #1 and Converter #2 can be got in Fig. 16. It can be reached that $i_{dc1}/i_{dc2} = R_{d2}/R_{d1} = 2$, so the proportional dc current sharing can be realized.

In the secondary control level, in order to flexibly regulate the communication delay in the experiment, a sample & hold block is employed in the experimental program. The output value of the secondary or tertiary controller is transferred to each converter at a low frequency by using the sampling & hold block. The output value of the secondary or tertiary controller at the beginning of each transmission interval is held until the next transmission starts. When t = 0, the secondary control level turns on. The effect of secondary controller is shown in Fig. 17. It can be seen that the deviation produced by the droop controller can be restored by secondary dc voltage controller. The load regulation is also tested by changing the load resistance from 400Ω to 133Ω, as shown in Fig. 18. It can be seen that by using the secondary control level, the dc bus voltage can be kept stable during the transient process of load step. The output waveform of the secondary controller is shown in Fig. 19. For comparison, the output waveform of the secondary controller without the sampling and hold block is also shown. It is seen from the stair-shape that the LBC is reached.

In the tertiary control level, similar to the secondary control level, the sample & hold unit is also employed to model the LBC. When the dc voltage is guaranteed to be within the acceptable range, the tertiary control is activated and the static switch for grid-connected operation is turned on. A bidirectional dc source should be provided to implement the dc grid. Therefore, a third ac-dc converter was adopted to achieve the above dc source. For safety consideration, the dc voltage reference value is lowered down to 600V in the dc grid-connected test. Fig. 20 shows the dc grid-connected current regulated by the tertiary PI controller. The dc current reference value is set to 0 – 1A – -1A – 0. When the dc grid-connected current is changing, the dc voltage waveform is exhibited in Fig. 21 accordingly. It is shown that dc current can be controlled to follow the reference value as expected. Meanwhile, the steady value of dc voltage is guaranteed to be within the acceptable range (570 V ≤ v_{dc} ≤ 630 V). The output waveform of the tertiary controller is exhibited in Fig. 22. It is shown from the stair-shape that the LBC is reached.

V. Conclusion

Different operation modes of a hybrid microgrid are discussed in this paper. Focusing on the interfacing converters between ac bus and dc bus, a dc-side hierarchical control system is designed and evaluated in this paper to analyze both standalone and grid-connected dc operation modes. In the decentralized primary control level of the hierarchical control system, ac current and dc voltage control are accomplished. For dc output load current sharing, droop controller is employed. Both equal and proportional current sharing are realized. In the secondary control level, with the common PI controller, dc bus voltage deviation caused by the droop control in the primary control level is restored. Meanwhile, common tertiary control level is involved to control the grid-connected current in the dc-side grid-connected operation. It has been demonstrated that each control level does not interfere with each other. Thus, the dynamics of different control levels are decoupled.

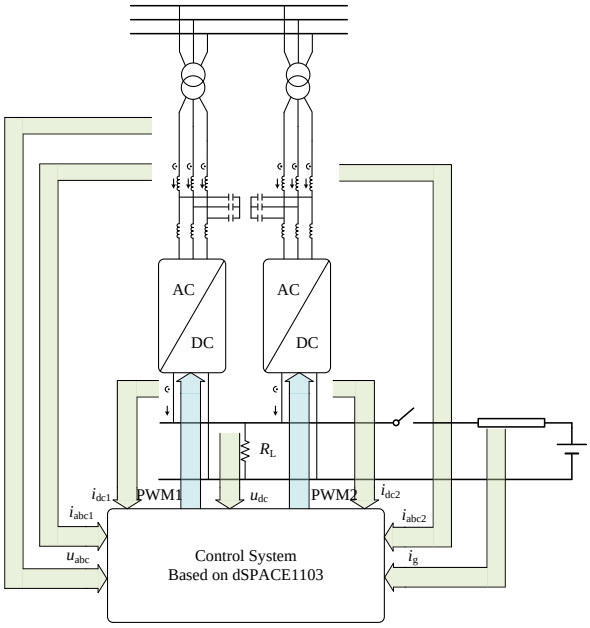

Fig. 11. System configuration of the prototype.

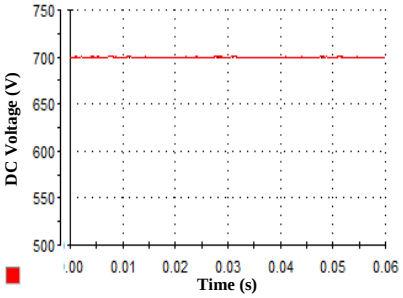

Fig. 12. Local dc voltage response.

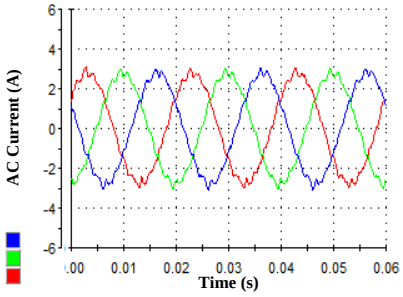

Fig. 13. Local ac current response.

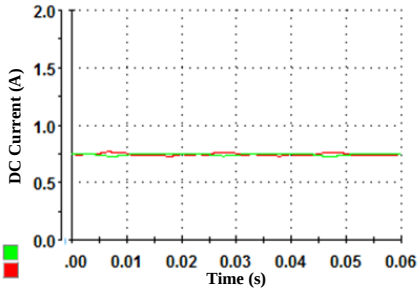

Fig. 14. Equal sharing of dc output current by droop control.

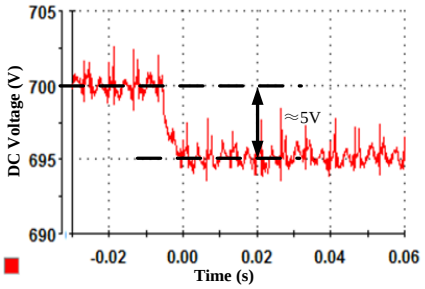

Fig. 15. DC voltage deviation produced by droop control.

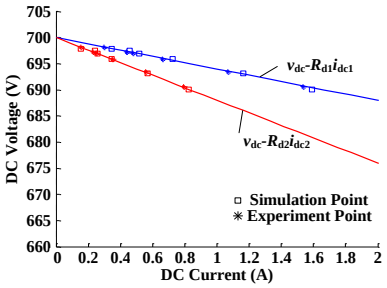

Fig. 16. Simulation and experimental test of dc current proportional sharing with different load currents.

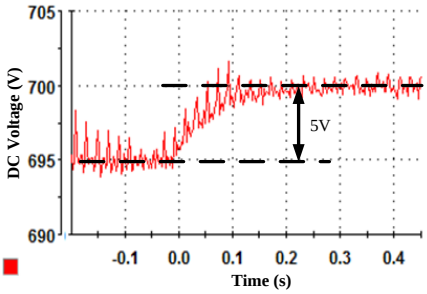

Fig. 17. DC voltage restoration of secondary control.

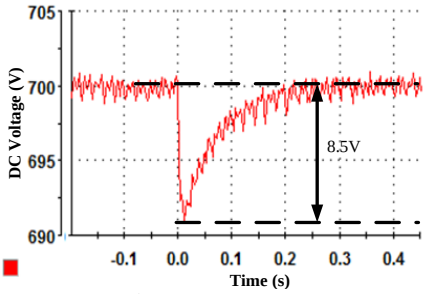

Fig. 18. Load step response of dc voltage secondary control.

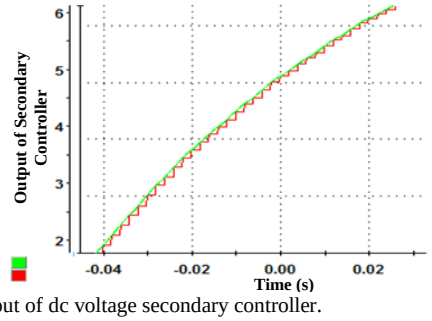

Fig. 19. Output of dc voltage secondary controller.

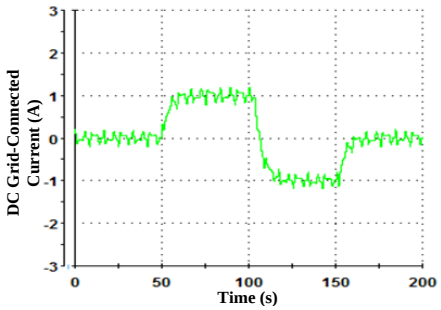

Fig. 20. DC grid-connected current with tertiary control.

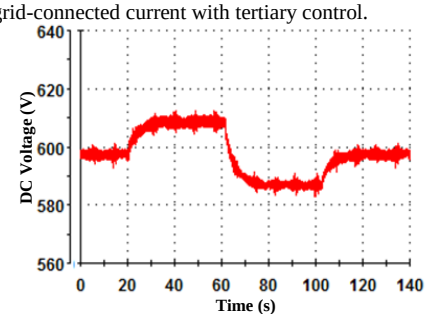

Fig. 21. DC voltage with tertiary control.

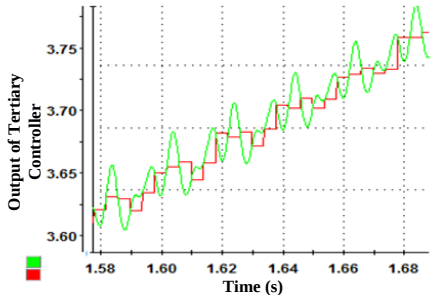

Fig. 22. Output of dc grid-connected current tertiary controller.

VI. References

[1] E. Bossanyi, *Wind Energy Handbook*. New York: Wiley, 2000.

[2] T. Markvart, *Solar Electricity*, 2nd ed. New York: Wiley, 2000.

[3] R. Lasseter, A. Akhil, C. Marnay, J. Stevens, J. Dagle, et al, "The certs microgrid concept - white paper on integration of distributed energy resources," *Technical report*, U.S. Department of Energy, 2002.

[4] F. Blaabjerg, Z. Chen and S. B. Kjaer, "Power electronics as efficient interface in dispersed power generation systems," *IEEE Trans. Power Electron.*, vol. 19, no. 5, pp. 1184-1194, 2004.

[5] J. M. Carrasco, L. G. Franquelo, J. T. Bialasiewicz, et al, "Power-electronic systems for the grid integration of renewable energy sources: a survey," *IEEE Trans. Ind. Electron.*, vol. 53, no. 4, pp. 1002-1016, 2006.

[6] C. T. Lee, C. C. Chuang, C. C. Chu and P. T. Cheng, "Control strategies for distributed energy resources interface converters in the low voltage microgrid," *in Proc. IEEE ECCE*, 2009, pp. 2022-2029.

[7] K. Kurohane, T. Senjyu, A. Yona, et al, "A hybrid smart AC/DC power system," *IEEE Trans. Smart Grid*, vol. 1, no. 2, pp. 199-204, 2010.

[8] X. Liu, P. Wang and P. C. Loh, "A hybrid AC/DC microgrid and its coordination control," *IEEE Trans. Smart Grid*, vol. 2, no. 2, pp. 278-286, 2011.

[9] Z. Ye, K. Xing, S. Mazumder, D. Borojevic and F. C. Lee, "Modeling and control of parallel three-phase PWM boost rectifiers in PEBB-based DC distributed power systems," *in Proc. IEEE APEC*, 2008, pp. 1126-1132.

[10] J. M. Guerrero, L. Hang and J. Uceda, "Control of distributed uninterruptible power supply systems," *IEEE Trans. Ind. Electron.*, vol. 55, no. 8, pp. 2845-2859, 2008.

[11] J. M. Guerrero, J. C. Vasquez, J. Matas, M. Castilla, et al, "Control strategy for flexible microgrid based on parallel line-interactive UPS systems," *IEEE Trans. Ind. Electron.*, vol. 56, no. 3, pp. 726-736, 2009.

[12] X. Lu, J. M. Guerrero, K. Sun, J. C. Vasquez. "An improved droop control method for dc microgrids based on low bandwidth communication with dc bus voltage restoration and enhanced current sharing accuracy," *IEEE Trans. Power Electron.*, to appear.

[13] Y. Li and Y. W. Li, "Power management of inverter interfaced autonomous microgrid based on virtual frequency-voltage frame," *IEEE Trans. Smart Grid*, vol. 2, no. 1, pp. 30-40, 2011.

[14] A. P. Martins, A. S. Carvalho and A. S. Araújo, "Design and implementation of a current controller for the parallel operation of standard UPSs," *in Proc. IEEE IECON*, 1995, pp. 584-589.

[15] J. Rajagopalan, K. Xing, Y. Guo and F. C. Lee, "Modeling and dynamic analysis of paralleled dc/dc converters with master-slave current sharing control," *in Proc. IEEE APEC*, 1996, pp.678-684.

[16] T. F. Wu, Y. K. Chen and Y. H. Huang, "3C strategy for inverters in parallel operation achieving an equal current distribution," *IEEE Trans. Ind. Electron.*, vol.47, no.2, pp.273-281, 2000.

[17] X. Sun, Y. S. Lee and D. H. Xu, "Modeling, analysis, and implementation of parallel multi-inverter systems with instantaneous average-current-sharing scheme," *IEEE Trans. Power Electron.*, vol.18, no.3, pp. 844-856, 2003.

[18] P. M. Kanabar, M. G. Kanabar, W. El-Khattam, T. S. Sidhu, et al, "Evaluation of communication technologies for IEC 61850 based distribution automation system with distributed energy resources," *in Proc. IEEE PES*, 2009, pp. 1-8.

[19] S. Anand, B. G. Fernandes and J. M. Guerrero, "Distributed control to ensure proportional load sharing and improve voltage regulation in low voltage DC microgrids," *IEEE Trans. Power Electron.*, vol. 28, no. 4, pp. 1900-1913, 2013.

[20] Y. Zhang and H. Ma, "Theoretical and experimental investigation of networked control for parallel operation of inverters," *IEEE Trans. Ind. Electron.*, vol. 59, no. 4, pp. 1961-1970, 2012.

[21] J. Anatory, N. Theethayi, R. Thottappillil, M. M. Kissaka, et al, "The influence of load impedance, line length, and branches on underground cable power-line communications (PLC) systems," *IEEE Trans. Power Del.*, vol. 23, no. 1, pp. 180-187, 2008.

[22] A. Pinomaa, J. Ahola and A. Kosonen, "Power-line communication-based network architecture for LVDC distribution system," *in Proc. IEEE Int. Symp. Power Line Commun. Appl.*, 2011, pp. 358-363.

[23] S. M. Ashabani and Y. A. I. Mohamed, "A flexible control strategy for grid-connected and islanded microgrids with enhanced stability using nonlinear microgrid stabilizer," *IEEE Trans. Smart Grid*, vol. 3, no. 3, pp. 1291-1301, 2012.

[24] D. Dong, T. Thacker, I. Cvetkovic, et al, "Modes of operation and system-level control of single-phase bidirectional PWM converter for microgrid systems," *IEEE Trans. Smart Grid*, vol. 3, no. 1, pp. 93-104, 2012.

[25] Z. Jiang and X. Y, "Hybrid dc- and ac-linked microgrids: towards integration of distributed energy resources," *in Proc. IEEE Energy 2030*, 2008, pp. 1-8.

[26] F. Shahnia, R. Majumder, A. Ghosh, G. Ledwich, et al, "Operation and control of a hybrid microgrid containing unbalanced and nonlinear loads," *Electric Power Systems Research*, vol. 80, no. 8, pp. 954-965, 2010.

[27] P. C. Loh, D. Li, Y. Chai and F. Blaabjerg, "Autonomous operation of hybrid microgrid with ac and dc subgrids," *IEEE Trans. Power Electron.*, vol. 28, no. 5, pp. 2214-2223, 2013.

[28] J. M. Guerrero, J. C. Vasquez, J. Matas, et al, "Hierarchical control of droop-controlled AC and DC microgrids - a general approach toward standardization," *IEEE Trans. Ind. Electron.*, vol. 58, no. 1, pp. 158-172, 2011.

[29] H. H. Huang, C. Y. Hsieh, J. Y. Liao and K. H. Chen, "Adaptive droop resistance technique for adaptive voltage positioning in boost DC-DC converters," *IEEE Trans. Power Electron.*, vol. 26, no. 7, pp. 1920-1932, 2011.

[30] C. Klumpner, M. Liserre and F. Blaabjerg, "Improved control of an active-front-end adjustable speed drive with a small dc-link capacitor under real grid conditions," in *Proc. IEEE PESC*, 2004, pp. 1156-1162.

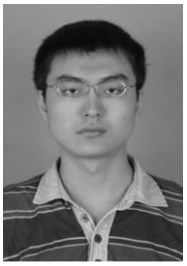

Xiaonan Lu (S'11) was born in Tianjin, China, 1985. He received the B.E. degree in 2008, in electrical engineering from Tsinghua University, Beijing, China, where he is currently working towards his Ph.D. degree. From Sep. 2010 to Aug. 2011 he was a guest Ph.D. student at Department of Energy Technology, Aalborg University, Denmark.

His research interests are control of power electronics interfacing converters for renewable generation systems and microgrids, multilevel converters, and matrix converters.

Mr. Lu is a student member of IEEE PELS Society.

Josep M. Guerrero (S'01-M'04-SM'08) received the B.S. degree in telecommunications engineering, the M.S. degree in electronics engineering, and the Ph.D. degree in power electronics from the Technical University of Catalonia, Barcelona, in 1997, 2000 and 2003, respectively. He was an Associate Professor with the Department of Automatic Control Systems and Computer Engineering, Technical University of Catalonia, teaching courses on digital signal processing, field-programmable gate arrays, microprocessors, and control of renewable energy. In 2004, he was responsible for the Renewable Energy Laboratory, Escola Industrial de Barcelona. Since 2011, he has been a Full Professor with the Department of Energy Technology, Aalborg University, Aalborg East, Denmark, where he is responsible for the microgrid research program. From 2012 he is also a guest Professor at the Chinese Academy of Science and the Nanjing University of Aeronautics and Astronautics. His research interests is oriented to different microgrid aspects, including power electronics, distributed energy-storage systems, hierarchical and cooperative control, energy management systems, and optimization of microgrids and islanded minigrids. Prof. Guerrero is an Associate Editor for the IEEE TRANSACTIONS ON POWER ELECTRONICS, the IEEE TRANSACTIONS ON INDUSTRIAL ELECTRONICS, and the IEEE Industrial Electronics Magazine, and an Editor for the IEEE TRANSACTIONS on SMART GRID. He has been Guest Editor of the IEEE TRANSACTIONS ON POWER ELECTRONICS Special Issues: Power Electronics for Wind Energy Conversion and Power Electronics for Microgrids; the IEEE TRANSACTIONS ON INDUSTRIAL ELECTRONICS Special Sections: Uninterruptible Power Supplies systems, Renewable Energy Systems, Distributed Generation and Microgrids, and Industrial Applications and Implementation Issues of the Kalman Filter; and the IEEE TRANSACTIONS on SMART GRID Special Issue on Smart DC Distribution Systems. He was the chair of the Renewable Energy Systems Technical Committee of the IEEE Industrial Electronics Society.

Kai Sun (M'12) was born in Beijing, China, 1977. He received the B.E., M.E., and Ph.D. degrees in electrical engineering all from Tsinghua University, Beijing, China, in 2000, 2002, and 2006, respectively. In 2006, he joined the faculty of Tsinghua University as a Lecturer of Electrical Engineering, where he is currently an Associate Professor. From Sep. 2009 to Aug. 2010 he was a Visiting Scholar at Department of Energy Technology, Aalborg University, Denmark.

He has authored more than 80 technical papers, including 9 international journal papers. His main research interests are power converters for renewable generation systems and AC motor drives. Dr. Sun received the Delta Young Scholar Award in 2013.

Juan C. Vasquez (M'12) received the B.S. degree in Electronics Engineering from Autonoma University of Manizales, Colombia in 2004 where he has been teaching courses on digital circuits, servo systems and flexible manufacturing systems. In 2009, He received his Ph.D. degree from the Technical University of Catalonia, Barcelona, Spain in 2009 at the Department of Automatic Control Systems and Computer Engineering, from Technical University of Catalonia, Barcelona (Spain), where he worked as Post-doc Assistant and also teaching courses based on renewable energy systems. Currently, he is an Assistant Professor at Aalborg University in Denmark. His research interests include modeling, simulation, networked control systems and optimization for power management systems applied to Distributed Generation in AC/DC Microgrids.

Remus Teodorescu (S'96-A'97-M'99-SM'02-F'12) received the Dipl.Ing. degree in electrical engineering from the Polytechnic University of Bucharest, Bucharest, Romania, in 1989 and the Ph.D. degree in power electronics from the University of Galaţi, Galaţi, Romania, in 1994.

In 1998, he joined the Power Electronics Section, Department of Energy Technology, Aalborg University, Aalborg, Denmark, where he is currently a Professor. He has more than 200 papers published, one book, entitled *Grid Converters for Photovoltaic and Wind Power Systems* (New York, NY, USA: Wiley, 2011), and five patents. His research interests include the design and control of power converters used in photovoltaics and wind power systems, grid integration with wind power, medium-voltage converters, HVDC/FACTS, and energy storage.

Dr. Teodorescu was an Associate Editor for IEEE TRANSACTIONS ON POWER ELECTRONICS LETTERS. He is the Chair of the IEEE Danish Joint Industrial Electronics/Power Electronics/Industry Applications Society Chapter. He is the Founder and Coordinator of the Green Power Laboratory, Aalborg University, focusing on the development and testing of grid converters for renewable energy systems. He is the Coordinator of Vestas Power Program, involving ten Ph.D. students and Guest Professors in the areas of power electronics, power systems, and energy storage.

(S'96–A'97–M'99–SM'02–F'12)

Lipei Huang was born in Jiangsu, China, 1946. He received the B.E. and M.E. degrees in electrical engineering from Tsinghua University, Beijing, China, in 1970 and 1982, respectively, and the Ph.D. degree from Meiji University, Tokyo, Japan, in 1996. In 1970, he joined the Department of Electrical Engineering, Tsinghua University. Since 1994, he has been a Professor in the Department of Electrical Engineering, Tsinghua University. In 1987, he was a Visiting Scholar of Electrical Engineering at the Tokyo Institute of Technology, for three months, and at Meiji University, Kawasaki, Japan, for nine months. He joined the research projects of K. Matsuse Laboratory, Department of Electrical Engineering, Meiji University, Kawasaki, Japan, as a Visiting Professor in 1993.

He has authored more than 100 technical papers and holds 7 patents. His research interests are in power electronics and adjustable-speed drives.

Prof. Huang received the Education Awards from the China Education Commission and Beijing People's Government in 1997. From 2001 to 2003 he was a Delta Scholar.